This article has been accepted for publication in a future proceedings of this conference, but has not been fully edited. Content may change prior to final publication.
Citation information: DOI10.1109/PAINE56030.2022.10014963, 2022 IEEE Physical Assurance and Inspection of Electronics (PAINE)

PCBA Image Analysis: A Comparison Of Visible, Infrared & X-ray Wavelengths

1st B. Malin
Brunel University London
London, United Kingdom
Ben.Malin@brunel.ac.uk

2nd T. Kalganova
Brunel University London
London, United Kingdom
Tatiana.Kalganova@brunel.ac.uk

3rd J. Danskins
Clyde Hyperspectral Imaging & Technology Ltd.
Glasgow, United Kingdom
JonD@clydehsi.com

4th J. R. Gilchrist
Clyde Hyperspectral Imaging & Technology Ltd.
Glasgow, United Kingdom
JohnRG@clydehsi.com

Abstract— **In the manufacture of printed circuit boards (PCB), various tests must be performed to ensure minimal defects are present in the final product. This is often done through visual inspection, using both X-rays as well as visible light, with X-rays often being superior due to the ability to capture internal features and defects. However, health and safety risks with X-rays lead to other, safer alternatives being desirable if they can provide comparable results. This work evaluates the visible differences between a range of near infrared (NIR) wavelengths using NIR hyperspectral imaging, as well as comparison to both X-ray and visible light images, to identify unique features that would benefit defect detection at each wavelength. Additionally, a small sample of NIR, visible light and X-ray PCBA images will be made public.**

Keywords—defect detection, infrared, X-ray, PCBA, hyperspectral imaging, image fusion

I. Introduction

PCBs (Printed Circuit Boards) are a commonplace means of connecting various electronic components together, once all components are connected it is referred to as printed circuit board assembly (PCBA). The components are typically connected using materials such as solder or copper. When these substances have gaps or breaks, disconnections will occur and can result in the PCBA performing differently than expected (or not at all). Due to the size of the PCB manufacturing industry, estimated to be worth $54.8 billion as of 2020 [1], it is of the utmost importance to reliably detect defects within PCBAs, to reduce both the cost of lost material but also the environmental impact.

Currently, the most ubiquitous manner of defect detection is in-circuit testing (ICT) this process tests a PCBA for resistances and capacitances across the board [2]. This is done using purpose-built fixtures equipped with various needles that are pressed onto a PCBA [2]. This methodology is commonplace due to its high level of accuracy, fast detection and the range of defects that are detectable, such as: open circuits, incorrect components and/or component values and broken traces [3]. However, ICT is specific to each PCBA that is being tested, leading to costs rising quickly when several unique PCBAs are needed for testing [3]. This methodology of detecting defects within a PCBA also has several issues associated with it, such as: having the ability to break a PCBA through electrostatic discharge (ESD), high initial costs, and recurring replacement costs [2][4]. Due to these shortcomings, much research has been conducted on replacement technologies, such as automated optical inspection (AOI) which is far cheaper to implement than ICT but cannot identify internal defects that ICT is capable of detecting [5], [6]. AOI utilizes imaging systems and deep learning to identify defects such as broken copper traces and solder. Another alternative that is often used is thermal imaging, which can identify defects such as solder shorts as well as component health [7]. However, a drawback of both optical and thermal imaging is the inability to show internal defects, a weakness which is not present within automated X-ray inspection (AXI). For this reason, AXI is a commonly used quality control tool within the PCB industry [5].

Whilst AXI is a powerful defect detection tool, the performance can suffer dependent on the size of the defect, as well as having additional drawbacks that relate to the associated risks of using X-rays [4]. The health and safety risks imposed upon X-ray imaging makes the implementation of AXI systems far more challenging, in addition to the high costs of purchasing the X-ray facilities in the first place, as well as the size and importability of X-ray machines. However, within the electromagnetic spectrum there are far more alternatives than just the commonly used optical, X-ray and thermal imaging methodologies. This is the motivation behind understanding what has been done before, as well as performing comparative analysis between the various imaging techniques.

This paper details and assesses commonly used PCBA analysis techniques in Section 2. In Section 3, the methodologies and setup used to capture the images in this paper are detailed. Section 4 provides and examines images of PCBAs captured at varying wavelengths. In Section 5 these images are compared and evaluated. Section 6 concludes the paper and provides future work.

The contributions of this paper are the following:

1) Providing and making public a small sample of PCBAs imaged over a wide range of wavelengths [8].

2) Identification of PCBA features visible to NIR wavelengths.

3) Provided a detailed comparison between applicability of various wavelengths for PCBA analysis.

This article has been accepted for publication in a future proceedings of this conference, but has not been fully edited. Content may change prior to final publication. Citation information: DOI10.1109/PAINE56030.2022.10014963, 2022 IEEE Physical Assurance and Inspection of Electronics (PAINE)

II. Related Work

Many nondestructive methodologies have been tested for PCBA defect detection applicability with a range of detectable defects for each technology. Some of the more varied methodologies will be reviewed to show what has already been achieved with PCB defect detection.

All techniques explored below in *Table 1* have shown success at detecting PCB defects. However, most techniques struggle with internal detection, excluding X-ray and ultrasound. But these methodologies have limitations, with ultrasound imaging not being suited for PCBA [4] and X-rays posing a health and safety risk. Additionally, research performed on ultraviolet defect detection shows that wavelengths close to visible light can provide unique benefit [11].

Thermal imaging of PCBAs is a commonly used procedure and has found major success within defect detection [5], [7], [9]. However, analysis using these infrared wavelengths has focused on the heat output and signatures of the components and boards themselves with minimal research done on the sub-thermal IR range, as well as to the spectral properties of PCB materials at these wavelengths. Or they require comparisons with healthy boards to detect defects [7], [9]. It is known that certain materials become transparent between specific wavelengths [12] and that some visually similar materials become distinct from one another at nonvisible light wavelengths [13], [14]. Due to the large range of wavelengths and techniques that succeed in finding unique features on or within PCBs, further evaluation of lesser tested methodologies is desirable. NIR Hyperspectral Imaging is an often-used inspection technique because it is nondestructive, noncontact, and nonionizing. It can also provide results that can identify both chemical and physical features of a target object [15]. Additionally, features present using these various techniques have not been compared. Thus, this work will analyze PCBAs at a range of wavelengths and compare and assess their visible features.

III. Methodology

To evaluate the differences in visible features across different imaging techniques, 3 PCBAs have been imaged using a visible light camera, X-ray machine and a NIR hyperspectral camera from Clyde HyperSpectral Imaging & Technology Ltd. The PCBAs were selected due to them each having unique and varied features and/or components present. The PCBAs are the Winnov Wavia R10, NVIDIA Jetson AGX Xavier and NVIDIA GeForce GT240.

The visible light images have been captured using a Nikon D90 DSLR camera at a resolution of 4288x2848. The X-ray images at 3840x3072 resolution, and the NIR hyperspectral images were captured at resolutions up to 863x617 pixels, across the spectral range from 950-1700nm and with spatial resolution of 0.22mm/pixel. NIR hyperspectral measurements can provide chemical, material and some depth information [12], [13], [15]. Due to the ability of X-rays to penetrate through most materials, images have only been taken from one side of each PCBA, as imaging from both sides resulted in mirrored images. Front and back images of all the PCBAs have been captured for both visible light and NIR hyperspectral wavelengths.

IV. Analysis

Preliminary analysis consists of manual visual inspection (MVI) to identify which features can and cannot be identified from the various imaging techniques.

A. Visible Light

From viewing the front-side of the visible light images and performing MVI, all external components can be clearly seen in *Figure 1*, along with copper trace and solder. These

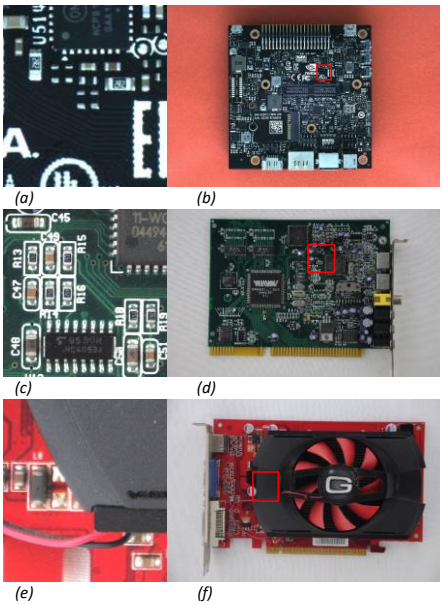

Figure 1 Visible light images of PCBAs (a) NVIDIA Jetson zoomed in, (b) NVIDIA Jetson full board, (c) Winnov Wavia R10 zoomed in, (d) Winnov Wavia R10 full board, (e) NVIDIA GT240 zoomed in, (f) NVIDIA GT240 full board

TABLE I. Nondestructive PCBA Defect Detection Methodologies

Author/Year	*Methodology*	*Defects*	*Limitations*
Zhang et al., 2022 [5]	X-ray – 3D AXI	Structural defects: solder, voids and shorts. Both external and internal	Noisy region of interest (ROI), health and safety risks.
Wang et al., 2022 [4]	Ultrasound	Internal and external flat bottom holes	Less effective on PCBA due to variety in material density, low variety of detectable defects.
Huang et al., 2020 [6]	Visible light	External structural defects	Inability to detect subsurface defects.
Alaoui et al., 2019 [7] Z. Dong and L. Chen 2019 [9]	Infrared Thermal Imaging	External structural defects and component health	Inability to detect subsurface defects.
Alaoui et al., 2018 [10]	Near EM field probing	Component related abnormalities as well as solder defects.	Measurements taken from 2mm away, so internal defects will be less accurate – especially on multilayer boards.
Hara et al., 1988[11]	Ultraviolet light	External structural defects	Inability to detect subsurface defects.

This article has been accepted for publication in a future proceedings of this conference, but has not been fully edited. Content may change prior to final publication.
Citation information: DOI10.1109/PAINE56030.2022.10014963, 2022 IEEE Physical Assurance and Inspection of Electronics (PAINE)

features can be more clearly seen in the zoomed in sections of the PCBA as shown in *Fig. 1a, c, d*.

B. *Infrared*

Using the hyperspectral camera, images were taken of the PCBAs at various wavelengths as shown below in *Fig. 2* and *Fig. 3*. The hyperspectral dataset was captured as reflection data and referenced to a "white calibration tile". The resulting data was then pre-processed using a Standards Normal Variance to remove variations in illumination affecting the result before being converted to absorbance values.

Between the three wavelengths shown there are minor differences in visible features, with the main distinction being the 1699nm wavelength's increased ability to image underneath silkscreen on the board (as demonstrated using a component label, marked in red for *Figs. 2d, 2e* and *2f*). Using Principal Component Analysis (PCA), the different materials can be distinctly shown in *Fig. 4*, with each color representing a different material. The corresponding spectral profiles for each material, shown in *Fig. 5a*, represent their absorbance spectra, with *Fig. 5b* correlating the profiles to their associated material. Both the front and the rear of the Winnov Wavia R10 were analyzed in this manner, with *Fig. 6a* displaying the board's rear spectral profile. With these spectral profiles it can be shown that identical materials have comparable spectra, and thus can be identified. For example, with plot 1 representing copper traces in both *Fig. 5a* and *Fig.*

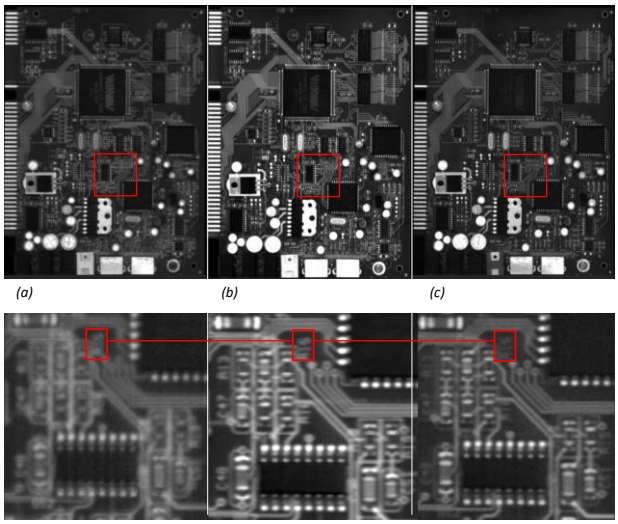

Figure 2 Winnov Wavia R10 front-side at (a) 970nm full board, (b) 970nm zoomed in, (c) 1340nm full board, (d) 1340nm zoomed in, (e) 1699nm full board, (f) 1699nm zoomed in

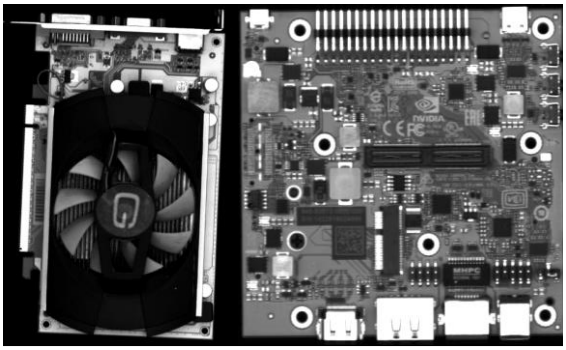

Figure 3 (a) NVIDIA GeForce GT240 1340nm, (b) NVIDIA Jetson 1340nm

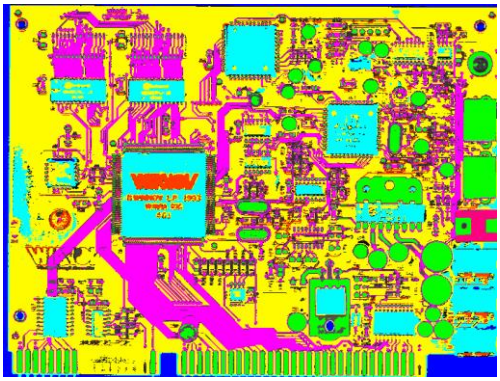

Figure 4 Principal Component Analysis on 1340nm image of the Winnov Wavia R10

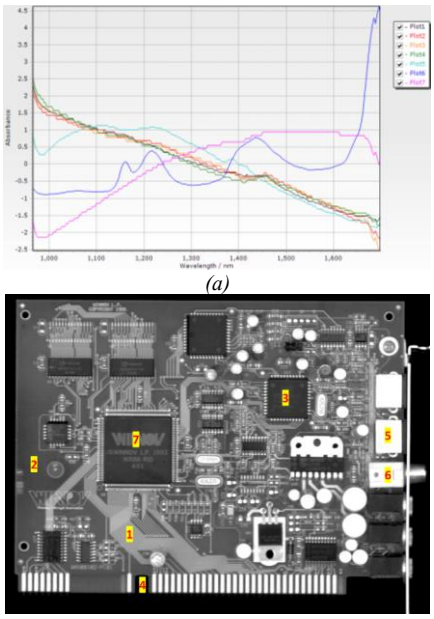

Figure 5 Winnov Wavia R10 front side (a) Spectral Profile, (b) 1340nm NIR image labelled with corresponding spectral plots

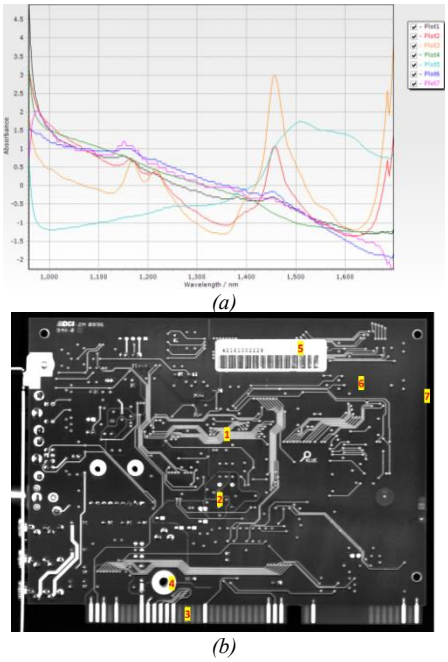

Figure 6 Winnov Wavia R10 rear side (a) Spectral Profile, (b) 1340nm NIR image labelled with corresponding spectral plots

This article has been accepted for publication in a future proceedings of this conference, but has not been fully edited. Content may change prior to final publication. Citation information: DOI10.1109/PAINE56030.2022.10014963, 2022 IEEE Physical Assurance and Inspection of Electronics (PAINE)

6a, their spectral profiles closely align, displaying PCBA material identification through spectral analysis.

Fig. 3 shows additional 1340nm images of the other two boards. *Fig. 3a* clearly showing an inability to image beneath the plastic present in the fan housing. *Fig. 3b* shows no internal features, but it is easy to observe the regions of the board which have used different materials.

C. X-ray

The X-rays shown in *Fig. 7* clearly show subsurface features, such as the internals of chips as well as copper trace and solder. The X-rays are also able to penetrate the plastic fan housing of the NVIDIA GeForce GT240 with ease and show the components beneath with minimal discoloration. However, the NVIDIA Jetson appears far more complex than the other two boards, and this is shown in *Fig. 7c* where the multitude of metal features on the rear side of the board obfuscates the front-side components. Although, this issue can be alleviated using more advanced X-ray imaging techniques, such as with 3D tomography whereby X-rays are taken at a variety of angles and rotations allowing a 3D model to be constructed. This methodology could show all the internal metal features at their respective depth, instead of overlaid on top of one another.

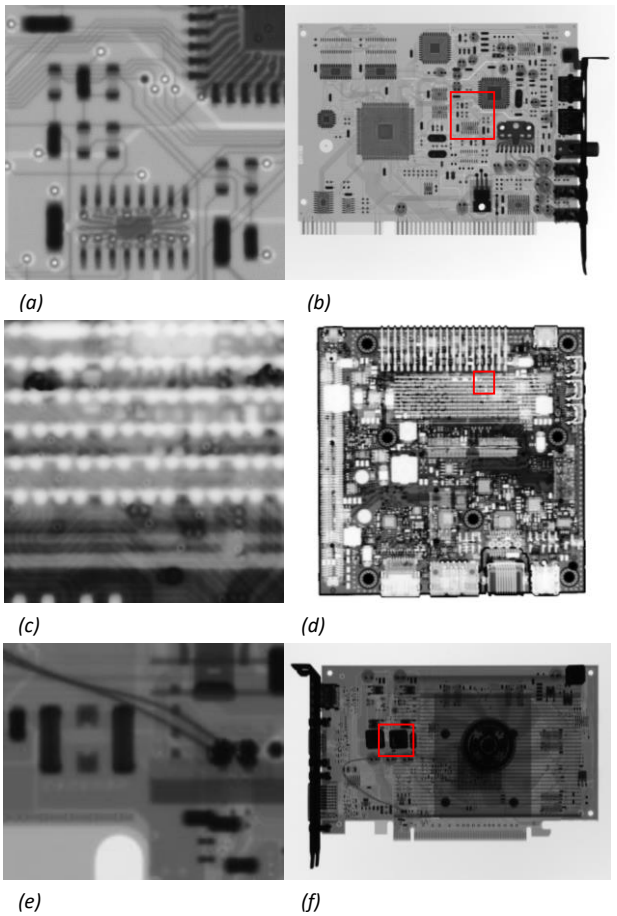

Figure 7 X-ray images of various PCBAs (a) Winnov Wavia R10 zoomed in, (b) Winnov Wavia R10 full board, (c) NVIDIA Jetson zoomed in, (d) NVIDIA Jetson full board, (e) NVIDIA GeForce GT240 zoomed in, (f) NVIDIA GeForce GT240 full board

V. COMPARISON

Fig. 8 showcases some of the differences in visible features between the tested wavelengths. Comparing visible to 1340nm, the main differences are the silkscreen (as shown in *Fig. 8b* compared to *Fig. 8d*) which becomes transparent at higher wavelengths. As well as the removal of very slight characteristics such as dust and minor scratches, leading to a cleaner image. In addition to this, the differences in visually similar materials are more noticeable using the 1340nm image, this is shown most prominently at the bottom of the board where the pins that are connected to trace are far more distinguishable than the other pins – which are also more clearly separated and distinguishable than their visible light counterparts, despite lower resolution.

Comparing the X-ray image to both other wavelengths shows a vastly different image, with far more observable features – owing to the high level of penetration found in X-rays. This allows the chip behind *Fig. 8b* and *Fig. 8d* to be observed as well as the internal construction of the chip. However, similarly to the visible light image, the X-ray image fails to distinguish between different materials as explicitly as the 1340nm image does, as evidenced once again by the pins at the bottom of the board.

Fig. 9 shows comparative images of the NVIDIA Jetson PCBA and provides a similar set of results to the Winnov Wavia R10. However, this set of images displays external

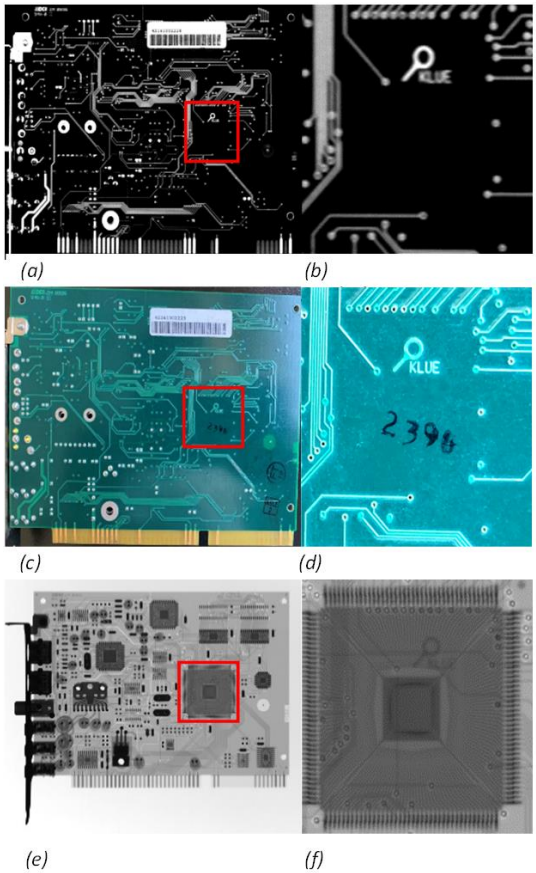

Figure 8 Comparison of imaging wavelengths on the Winnov Wavia R10's rear-side (a) 1340nm full board, (b) 1340nm zoomed in, (c) visible light full board, (d) visible light zoomed in, (e) X-ray full board, (f) X-ray zoomed in

This article has been accepted for publication in a future proceedings of this conference, but has not been fully edited. Content may change prior to final publication. Citation information: DOI10.1109/PAINE56030.2022.10014963, 2022 IEEE Physical Assurance and Inspection of Electronics (PAINE)

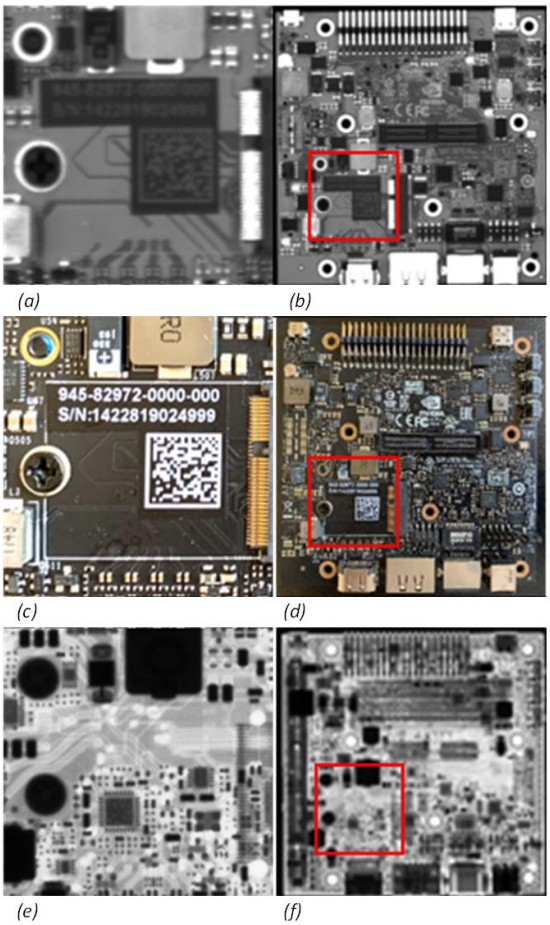

Figure 9 Comparison of imaging wavelengths on the NVIDIA Jetson (a) 1340nm zoomed in, (b) 1340nm full board, (c) visible light zoomed in, (d) visible light full board, (e) X-ray zoomed in, (f) X-ray full board

components that were not found on the Winnov Wavia R10's rear-side. All sets of images can uniquely identify capacitors and resistors. However, with the X-ray images there are a lot of components on the board's rear-side which is making the identification of front-side components far more difficult, an issue that the other methodologies do not face. But this is an issue that would be remedied with the more advanced X-ray tomography. Once again, the 1340nm wavelength can clearly distinguish between different, visually similar, materials. This is most noticeable when comparing *Fig. 9a* with *Figs. 9c* and *9d* where the 1340nm image distinctly shows that different materials have been used, as is seen by the different shading around the serial number compared to the adjacent patch of PCB. This is far less obvious to observe with visible light and impossible to see through the X-ray image.

Computer aided comparison has also been demonstrated in *Fig. 10* where alignment, equalization and subtraction has been performed between images of differing wavelengths. *Fig. 10a* shows the 1340nm image of the Winnov Wavia R10 with a visible light image subtracted from it. Distinctions between the two images are now clearer, with metallic surfaces (such as copper trace and pins) being bright and clearly visible, as well as some text and silkscreen being more visible. This shows the disparity between the images used, caused by the NIR image penetrating the silkscreen as well as exposing metal components more than the visible light. *Fig. 10b* shows the image subtraction results from subtracting an X-ray image from a visible light image. This has resulted in

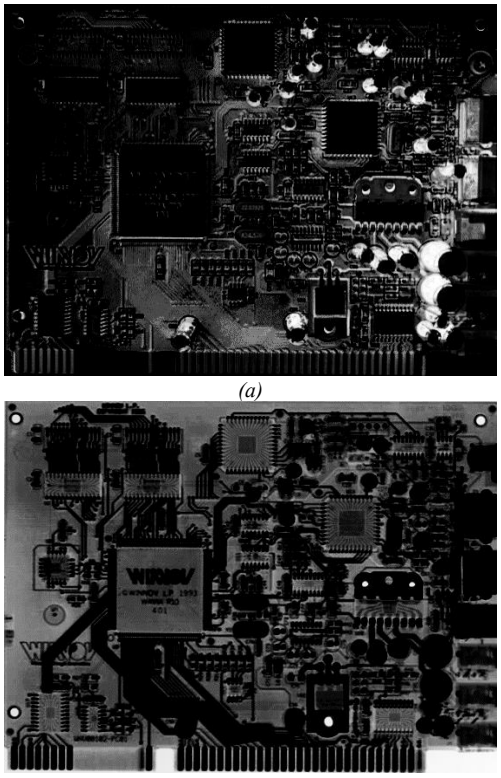

Figure 10 Winnov Wavia R10 Image subtraction (a) 1340nm minus visible light, (b) visible light minus X-ray

visually fusing many of the features, allowing the internal features of several components to be visible alongside the features that are invisible to X-ray – such as text. Utilizing these images together has the potential to aid classification and defect detection, due to the presence of additional features within a single image.

However, when the subtraction is performed in grayscale it is not easily distinguishable which features are correlated to which wavelength. Thus, to better demonstrate the differences between each image pair, one has been converted to redscale and both have had transparency effects applied, in addition to the alignment and equalization. This can be seen in *Figure 11*, displaying this methodology for the *NVIDIA Jetson*. *Fig. 11a* clearly shows the text, silkscreen, and other features only visible to the visible light wavelengths in redscale alongside the numerous X-ray specific features that can be viewed due to the superior penetration offered by X-rays.

This technique was also used to compare the 1340nm wavelength to the visible light wavelength, shown in *Fig. 11b*. These images are far more alike than either are to the X-ray images, causing most of the outputted image to be tinted red. However, it is the areas of brighter red, or lack thereof, that are of note. The areas of brighter red signify a higher intensity at the 1340nm wavelength, which can be seen on metallic components. Whereas the darker areas signify the opposite, allowing for the composite image to maintain the 1340nm wavelength's superior ability to distinguish material differences. This can be evidenced when comparing *Fig. 11b* to *Figs. 9a* and *9c*, with the composite image clearly defining the different materials through its shading – due to the 1340nm having varying light intensities for the different materials, which can be imprinted upon the monochromatic

This article has been accepted for publication in a future proceedings of this conference, but has not been fully edited. Content may change prior to final publication. Citation information: DOI10.1109/PAINE56030.2022.10014963, 2022 IEEE Physical Assurance and Inspection of Electronics (PAINE)

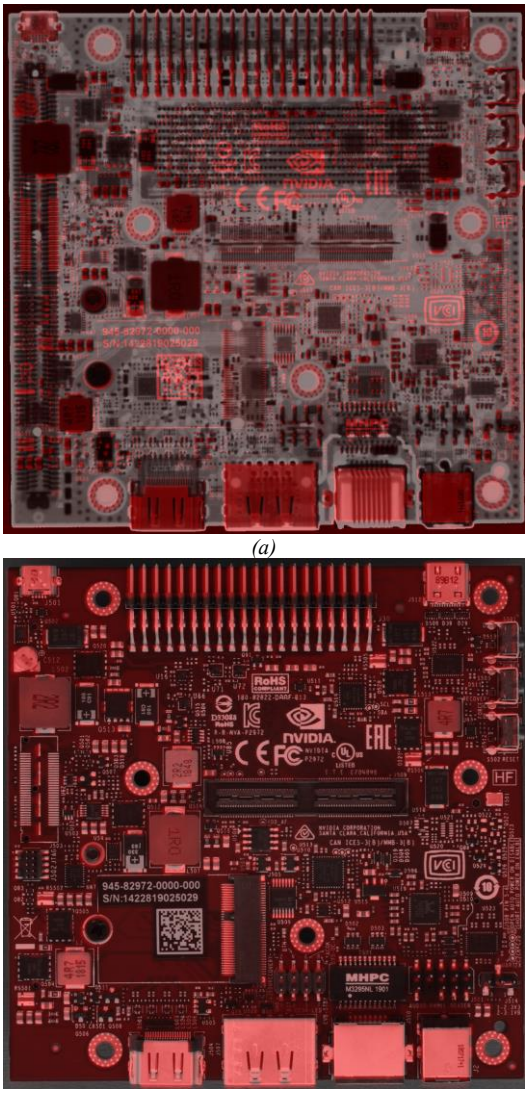

(a)

(b)

Figure 11 NVIDIA Jetson Image superpositioning (a) visible light (redscale) and X-ray (grayscale), (b) 1340nm (redscale) and visible light (grayscale)

visible light region. Additionally, this technique allows the unique, but low resolution, 1340nm wavelength features to be more clearly viewed at a higher resolution, through utilization of the visible light image.

Additional images displaying the comparison between various wavelengths and boards can be found within the published dataset, demonstrating both comparative methodologies studied.

VI. CONCLUSION AND FUTURE WORK

NIR hyperspectral imaging has unique benefits to both X-ray and visible light imaging, with the most noticeable difference being its ability to distinguish between visually similar materials. This can be done using a board's unique spectral profile, or through IR images, with the application of PCA clearly defining different materials within an image. In addition to this, it can image beneath minor elements on a PCBA (specifically silkscreen, but also certain types of plastic). However, this does not allow it to capture internal PCBA features as the X-ray images are able to do. Due to this, images taken between 970nm and 1700nm would be superior in defect detection to visible light images in the event when copper trace or solder is covered by silkscreen, or if the defect is due to an incorrect material having been used in the board's construction. The only benefit of using visible light images, excluding lower installation costs, is from potentially relevant color data. However, this is unlikely to be informative of a defect, and hyperspectral images would be able to distinguish between the colors anyway – provided they are of different materials. Although, using image subtraction or superpositioning to fuse features unique to specific wavelengths together in a composite image has the potential to mitigate some of the weaknesses within both visible and NIR light. These composite images also have the capability to improve both classification and defect detection, due to the presence of features independent to specific wavelengths within a singular image.

Further analysis on the different materials that can be identified with NIR is desirable, as well as improving the image quality through increasing SNR. This should allow for more comprehensive analysis on the identifiable features of a PCBA NIR image. Additionally, the use of a board's spectral profile to classify both the board and its material composition is an area for which future work can be performed.

ACKNOWLEDGEMENTS

This research is sponsored by Air Force Defense Research Sciences Program, GRANT13113392.

REFERENCES

[1] Wood, L., 2022. Global Printed Circuit Boards (PCBs) Market Report 2022: Market to Surpass $75 Billion by 2027 - Digital Transformation Catalyzed by the Pandemic Provides the Perfect Platform for Growth. [online] GlobeNewswire. Available at: <https://www.globenewswire.com/en/news-release/2022/06/16/2463963/28124/en/Global-Printed-Circuit-Boards-PCBs-Market-Report-2022-Market-to-Surpass-75-Billion-by-2027-Digital-Transformation-Catalyzed-by-the-Pandemic-Provides-the-Perfect-Platform-for-Growth.html> [Accessed 1 August 2022].

[2] M. Jeon, S. Yoo, and S. W. Kim, "A Contactless PCBA Defect Detection Method: Convolutional Neural Networks with Thermographic Images," *IEEE Transactions on Components, Packaging and Manufacturing Technology*, vol. 12, no. 3, pp. 489–501, Mar. 2022, doi: 10.1109/TCPMT.2022.3147319.

[3] J. E. M. Martín, A. S. Nevado, and A. V. Martínez, "Low cost programmable modular system to perform In-Circuit Test (ICT): Full development of the hardware, software and mechanics of an ICT machine," Aug. 2016. doi: 10.1109/TAEE.2016.7528359.

[4] F. Wang *et al.*, "Quantitative imaging of printed circuit board (PCB) delamination defects using laser-induced ultrasound scanning imaging," *Journal of Applied Physics*, vol. 131, no. 5, Feb. 2022, doi: 10.1063/5.0077766.

[5] Q. Zhang *et al.*, "Deep learning based solder joint defect detection on industrial printed circuit board X-ray images," *Complex & Intelligent Systems*, vol. 8, no. 2, pp. 1525–1537, Apr. 2022, doi: 10.1007/s40747-021-00600-w.

[6] W. Huang, P. Wei, M. Zhang, and H. Liu, "HRIPCB: a challenging dataset for PCB defects detection and classification," *The Journal of Engineering*, vol. 2020, no. 13, pp. 303–309, 2020, doi: 10.1049/joe.2019.1183.

[7] N. E. B. Alaoui, P. Tounsi, A. Boyer, and A. Viard, "Detecting PCB Assembly Defects Using Infrared Thermal Signatures," Toulouse, France, 2019.

[8] Ben Malin, Tatiana Kalganova, Sebelan Danishvar, and Dominic Sanderson, "PCBA X-ray and Visible Light Small Dataset.", 2022. Kaggle, [Online]. Available: https://www.kaggle.com/ds/2354159. doi: 10.34740/KAGGLE/DS/2354159

[9] Z. Dong and L. Chen, "Image registration in PCB Fault Detection Based on Infrared Thermal Imaging; Image registration in PCB Fault Detection Based on Infrared Thermal Imaging," 2019.

[10] N. E. B. Alaoui *et al.*, "New defect detection approach using near electromagnetic field probing of high density PCBAs," *Microelectronics Reliability, Elsevier*, pp. 288–293, 2018, doi: 10.1016/j.microrel.2018.07.090ï.

[11] Y. Hara, H. Doi, K. Karasaki, and T. Iida, "A System for PCB Automated Inspection Using Fluorescent Light," *IEEE Transactions on Pattern Analysis and Machine Intelligence*, vol. 10, no. 1, pp. 69–78, 1988, doi: 10.1109/34.3868.

[12] K. Sato, Y. Kurosaki, T. Saito, and I. Satoh, "Laser welding of plastics transparent to near-infrared radiation. ," *Proceedings of SPIE - The International Society for Optical Engineering*, 2002.

[13] F. Ou *et al.*, "Plastic sorting with an integrated NIR spectral sensor," Jun. 2021. doi: 10.1109/CLEO/Europe-EQEC52157.2021.9542482.

[14] A. C. Karaca, A. Ertürk, M. Kemal Güllü, M. Elmas, and S. Ertürk, "Kizilötesi hiperspektral görüntüleme sistemi ile plastik atiklarin ayristirilmasi," 2013. doi: 10.1109/SIU.2013.6531170.

[15] G. Bonifazi, G. Capobianco, and S. Serranti, "Hyperspectral imaging applied to the identification and classification of asbestos fibers," Dec. 2015. doi: 10.1109/ICSENS.2015.7370458.